© 2017 IJSRSET | Volume 3 | Issue 8 | Print ISSN: 2395-1990 | Online ISSN : 2394-4099
Themed Section : Science and Technology

Thermal Evolution of Zinc Aluminate Spinel Nanoparticles Prepared by Coprecipitation Technique

Dr. Shyam Sunder* and Dr. Wazir Singh
Department of Applied Science and Humanities, Ch. Devi Lal State Institute of Engineering & Technology
Panniwala Mota, Sirsa, India
*Corresponding author: shyampph@yahoo.com

ABSTRACT

Zinc aluminate (ZnAl2O4) has the spinel structure and has been used as a catalyst itself, catalyst support, catalysis and in many catalytic reactions, such as cracking, dehydration, hydrogenation, dehydrogenation reactions, the phosphor host etc. At calcination temperature 700°C (4h), an intermediate phase (γ-Al_2O_3, a rock salt type structure) of cubic $ZnAl_2O_4$ was formed. At calcination temperature 800°C (4h), interfacial interaction between high reactive decomposed products γ-Al_2O_3 and ZnO and their mixing at molecular level yielded $ZnAl_2O_4$ face-centred cubic spinel nanopowder via distribution of cations among the interstitial sites. It is observed that calcination enhances the crystallinity and transmission of the spinel; and also controls dislocation density and amount of stress at the surface and hence yields the strength of the material. A single phase $ZnAl_2O_4$ face centred cubic spinel nanopowder (grain size ~ 25 nm) can be obtained by using co-precipitation method followed by thermal treatment at temperature 900°C for 4h, in air.

Keywords : Zinc aluminate, Nanoparticle, Coprecipitation, Structure Characterization

I. INTRODUCTION

Spinel-type mixed oxides are non-toxic, inexpensive, very stable materials with strong resistance to acids and alkalis, and they have high melting points and relatively high surface areas [1-2]. The general structure formula of the spinel-type mixed oxides may be represented as $(A_{(1-x)}B_x)^{tet}[A_xB_{(2-x)}]^{oct}O_4$, where *x, tet* and *oct* is the inversion parameter/degree of disorder, tetrahedral octahedral. If *x* is 0, the cations are completely ordered onto the two cation sites, the structural formula is $(A)^{tet}[B_2]^{oct}O_4$, and the spinel is said to have the "normal" cation distribution. The opposite extreme occurs if *x* is 1, corresponding to $(B)^{tet}[AB]^{oct}O_4$, in that case, the spinel is said to have the "inverse" cation arrangement [3]. A remarkable feature of spinel structure is that it is able to form virtually unlimited number of solid solutions. This means that the composition of spinel can be varied significantly without altering the basic crystalline structure. Depending on cation distribution, a spinel can be normal, inverse, or mixed. In a normal spinel (e.g., $NiCr_2O_4$ and $ZnFe_2O_4$) the tetrahedral and octahedral sites are occupied by divalent and trivalent cations, respectively. If tetrahedral sites are completely occupied by trivalent cations and the octahedral sites are shared by both divalent and trivalent cations, it is an inverse spinel (e.g., $NiFe_2O_4$ and γ-Fe_2O_3). However, most spinels are mixed spinels (e.g. $MnFe_2O_4$) in which divalent and trivalent cations occupy both tetrahedral and octahedral sites.

Among various inorganic spinels, Zinc aluminate, a mixed oxide of aluminium and zinc, is a naturally available mineral commonly called as gahnite with a normal spinel structure in which zinc and aluminium cations occupied their natural sites: A and B interstitial sites. The $ZnAl_2O_4$ spinel structure is crystalline and belongs to the F3dm space group with a cubic symmetry. Each unit cell is composed of eight AB_2O_4 patterns. The unit cell contains 32 oxygen atoms, which form 64 tetrahedral sites and 32 octahedral sites. In the direct spinel structure, only 8 of the tetrahedral sites (Wyckoff positions 8*a* (⅛, ⅛, ⅛)) and 16 of the octahedral sites (Wyckoff positions 16*d* (½, ½, ½)) are respectively occupied by A and B cations. The oxygen atoms fully occupy the 32e positions. Nevertheless, in the composition of $ZnAl_2O_4$, non-negligible equal proportions of A (Zn^{2+}) in the 16*d* Wyckoff position and B (Al^{3+}) in the 8*d* position can be reached to interstitial sites of $ZnAl_2O_4$. It is well known fact that $ZnAl_2O_4$ is a wide band gap (3.8 eV) semi-conductor; due to which this material does not absorb wavelengths higher than 325 nm [4-5]. $ZnAl_2O_4$ can also be used as a second phase in glaze layers of white ceramic tiles to improve wear resistance and mechanical properties and to preserve whiteness as a ceramic material similar to magnesium aluminate ($MgAl_2O_4$) [6]. This spinel solid can be considered as the non-magnetic counterpart of zinc ferrite and an ideal template to test the hypothesis on the migration of zinc ions to the B sites as a consequence of the size reduction as the standard property. Thus it is a suitable white host matrix for doping with phosphor cations for photo-emission applications. It can be used as a catalyst itself, catalyst support, and catalysis and in many catalytic reactions, such as cracking, dehydration, hydrogenation and dehydrogenation reactions [7-12], since it has a high thermal stability, low acidity, hydrophobic behaviour. It can also be used as a transparent conductive oxide, as a sintering aid reagent for alumina ceramic and for its dielectric properties. Moreover, it has a strong metal-support interaction preventing e.g. platinum and platinum/tin to sinter. Consequently, one of the most extensively studied properties of doped $ZnAl_2O_4$ compounds is their photoluminescence. Zinc aluminates resembles zinc ferrite structurally, and it has been found recently that zinc ferrite in the nano-regime show anomalous magnetic properties, because zinc ions instead of occupying tetrahedral (A) sites, partially occupies octahedral (B) sites, when prepared in the nano-regime [13].

Zinc aluminate is normally synthesized via a solid-state reaction of zinc and aluminium oxides above 600ºC [14-21]; such as sol-gel methods [22-25], hydrothermal [26-29] and coprecipitation with several organic precursors etc [14, 16, 30-33]. Zinc aluminate powder was synthesised by heating equimolar ZnO and Al_2O_3 powders in alkaline chlorides (LiCl, NaCl or KCl). Literature reveals that the effect of processing factors (e.g., heating temperature, salt type and particle size of Al_2O_3 powder) were examined on the formation of $ZnAl_2O_4$ and observed that the synthesized $ZnAl_2O_4$ grains are close in size and shapes of the original Al_2O_3 powders [34]. Zinc aluminate with the spinel crystal structure was obtained at low temperatures by the sol-gel method and effect of heat treatment on the particle size of zinc aluminate was also discussed. Using Zn:ethylenediamine complex, as a precursor and diethylene glycol monoethyl ether and citric acid as chelating ligand and solvent [35], $ZnAl_2O_4$ nanoparticles (size ~ 6 nm) were synthesised around temperature 550ºC by modified sol-gel route [36]. $ZnAl_2O_4$ spinels were also prepared by different techniques (ceramic method, mechano-chemical synthesis and coprecipitation) and found that the coprecipitation synthesis seems to be appropriate for synthesis of solids with the adequate characteristics for application as support of metallic catalysts for *n*-butane dehydrogenation; because of high chemical purity, higher specific area and an adequate acidity [37].

Coprecipitation is one of the simplest techniques for preparing nanoparticles of numerous inorganic materials. In this simple and inexpensive method, salts of the required metals are dissolved in water and coprecipitated by adding a precipitating agent. In fact, the precipitates obtained are solid solutions that contain the cations mixed together, essentially on an atomic scale. Because of the high degree of homogenization, much lower temperatures are sufficient for the reaction to occur. Using inorganic solids as heterogeneous catalysts, Spinel-type $ZnAl_2O_4$ nanoparticles prepared by the coprecipitation method was studied and the reaction involved and its application as a heterogeneous catalyst for the efficient acetylation of alcohols, phenols and amines under mild conditions (solvent-free, atmospheric pressure, room temperature) was demonstrated [38].

Recent investigations on $ZnAl_2O_4$ spinels explore how properties of systems can be modified by controlling the cation distribution in oxide spinels for electronics and electrical engineering applications. The distribution of cations in a simple end-member oxide spinel significantly alters properties of the spinels [39]. Qualitatively, such behaviour can be related to two factors: (a) difference in lattice parameters or ionic sizes and (b) the variation in cation distribution across the solid-solution series. Non-linear structural property has been used as electric/electronic circuit protector (varistors). The temperature dependence of the cation distribution in spinel is of particular interest. With increasing calcinations temperature, degree of disorder (x) was found 0.32 and 0.36 at temperature 613°C and 1195°C. The change in x over this temperature range is very small. A quantitative model incorporating these two factors was proposed by O'Neill and Navrotsky (1983, 1984) [37-38]. It includes the size-difference term as a regular solution parameter whose magnitude depends on the difference in radii of ions being mixed. The current interests are focused on obtaining accurate measurements of the equilibrium cation distribution as a function of variables such as temperature and composition, with a view to building and testing thermodynamic models, investigating the relationship between cation distribution and also the physical and thermodynamic properties of multi-component spinel solid solutions.

In the light of above discussion, the coprecipitation method is selected for the preparation of $ZnAl_2O_4$ nanopowders and the effect of thermal treatment on the structural change of prepared ceramic spinel $ZnAl_2O_4$ has been investigated in detail. The possibility of thermal induced order-disordered spinel structural phase transformation in cubic zinc aluminate nanopowder is explored. The advantage of the powder method over the use of single crystals is that the spinel can be synthesized under conditions which are the optimum for achieving the desired stoichiometry, without the necessity of growing large crystals.

II. EXPERIMENTAL

The zinc aluminate cubic spinel nanopowders were prepared by coprecipitation method. The high purity reagents $Zn(NO_3)_2{\cdot}6H_2O$ (99.99% purity Sigma Aldrich ACS grade), $Al(NO_3)_3{\cdot}9H_2O$ (99.99% purity Sigma Aldrich ACS grade) and ammonia solution (28%, Sigma Aldrich ACS grade) were used to prepare magnesium aluminate cubic spinel nanopowders. A 0.2M solution of the nitrates was prepared in double distilled water, with Zn:Al (molar ratio)= 1:2. Both the solutions of nitrates were mixed together for homogenization. The precursor was prepared by slowly adding the mixed salt solution into the ammonia solution under rigours stirring.

The pH was maintained around 8-9 and reaction temperature was kept at 60°C. The precursors, so obtained, were washed many times with an excess of double distilled water. The washed precipitates of precursor were dried for 24 hrs at 100°C in an oven in the presence of air. The solid obtained was

grinded in agate mortar pestle to obtain fine powder. Furthermore, powdered samples were calcined at different temperatures 600°C, 700°C, 800°C and 900°C for four hours (heating rate 10°C min^{-1}) in air (Figure 1).

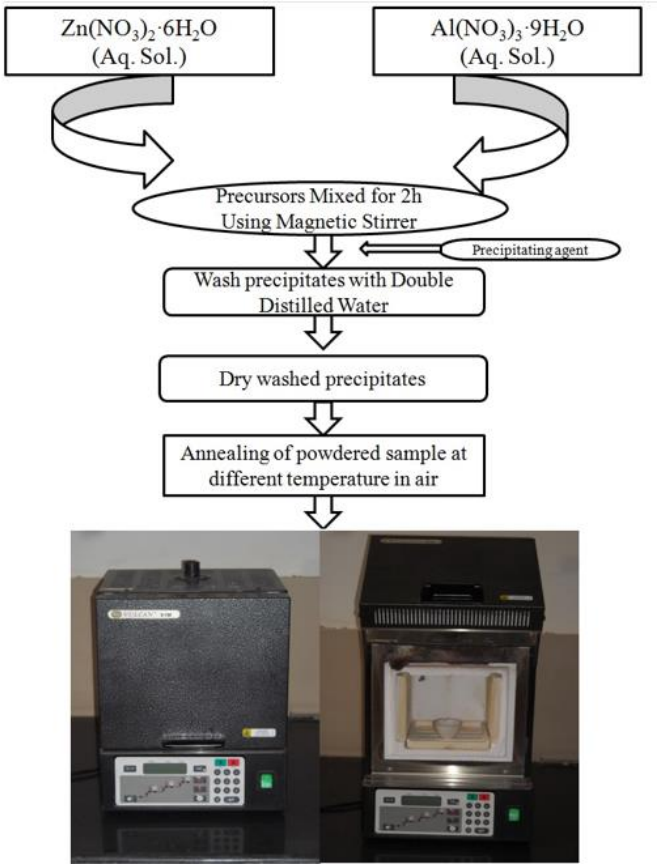

Figure 1 : Synthesis scheme of the Zinc aluminate powder

Thermo Gravimetric and Thermo Gravimetric Analysis (TGA-DTG-DTA) were carried out by model SII 6300 EXSTAR. X-ray diffraction experiments were performed at room temperature in a Rigaku Miniflex-II instrument using CuKα radiation (λ = 1.5406 Å), generated at 30 kV and a current of 15 mA. The Joint Committee on Powder Diffraction Standards (JCPDS)-International center for diffraction data cards were referred for the determination of the phases developed. Fourier Transform Infrared Spectrum was taken on Perkin-Elmer Spectrum RX1 Spectrophotometer. The morphology and microstructure of the powders was studied by scanning electronic microscope (SEM), with a Nova NanoLab 200 FEG-SEM/FIB, equipped with energy dispersive spectroscopy (EDS).

III. RESULTS AND DISCUSSION

3.1Thermogravametric Analysis (TGA-DTG-DTA)

The Thermo Gravimetric Analysis (TGA and DTG) patterns of the precursor powder are presented in Figure 2. The TGA curve shows a major weight loss of the sample at four different temperature range 50-100°C, 101-265°C and 266-500°C and 501-800°C. Between temperature 50 and 100°C (first stage), the weight loss is 7.0% and it is due to evaporation of physically adsorbed water molecules. In the temperature range 101-265°C (second stage), the weight loss is nearly 25% and this could be due to decomposition of precursors.

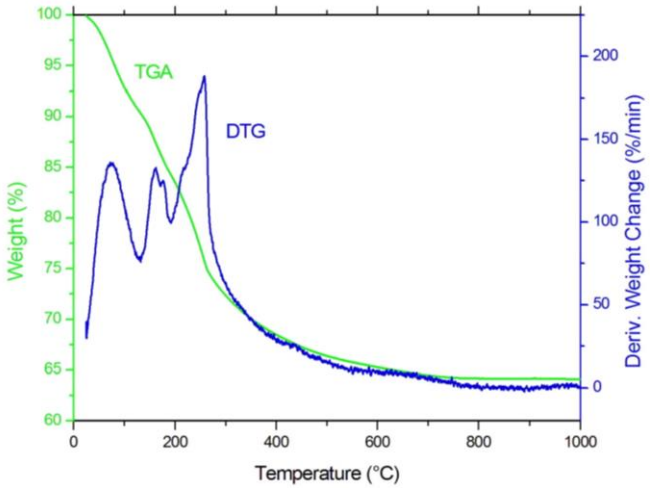

Figure 2 : TGA-DTG curves of the Zinc aluminate powder.

Between the temperature 266 and 500°C (third stage); the rate of weight loss is almost constant, indicating an intermediate structure is formed. Over a temperature range 501-800°C, the weight loss is very small means an intermediate structure is formed. Finally, between temperature 801 and 1000°C, TGA curve exhibits negligible weight loss in the sample, indicating a stable structure of the zinc aluminium oxides is formed. The TGA analysis reveals that the total weight loss in the prepared powder is about 36%, implies that the final product

with good yield could be obtained by coprecipitation method.

In the DTG profile, peaks at 78°C and 162°C correspond to the release of free bound water and loss of crystal water from a new compound originated by the hydration process, respectively. A strong peak in DTG curve is observed at 257°C, which ascribes the decomposition of residual nitrates and moisture. This finding suggests decomposition reaction of the hydroxide of zinc and aluminium precursor. TGA experiments did not give additional information about the $ZnAl_2O_4$ spinel formation at high temperatures in all cases, probably due to the slowness of the transformation process of the precursors into the spinel.

However, this fact could cause the small weight losses observed in TGA experiments at high temperatures. Therefore, we selected 800°C as the calcination temperature for preparing the $ZnAl_2O_4$ spinel.

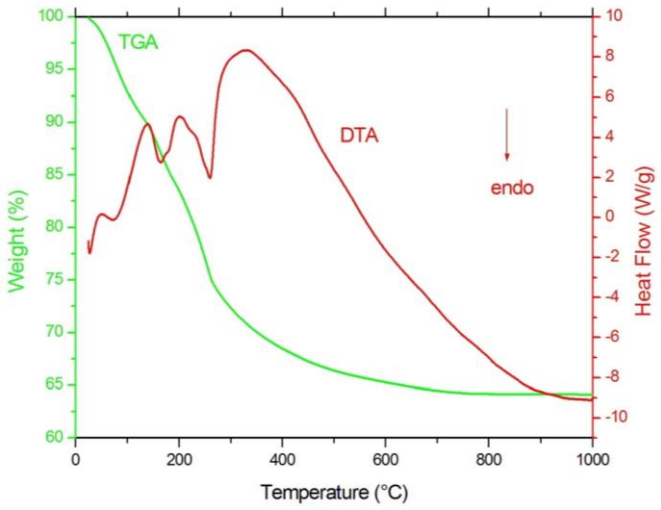

Figure 3 : TGA-DTA curves of the Zinc aluminate powder.

Figure 3 shows DTA and TGA results of the as-prepared sample. The DTA curve shows an endothermic reaction below 100°C (typically at 74°C) which is attributed to the loss of the remaining adsorbed water. A peak at about 163°C, this could be due to the endothermic reaction by the decomposition of the hydroxide of zinc and aluminium. This agrees with the weight loss given by TGA data as shown in Figure 2. Also, in Figure 3, another endothermic peak at about 259°C is found and is assumed to be due to the formation of $ZnAl_2O_4$ particles. A broad exothermic peak is observed in the range 260-350°C, this attributes to the crystallization of $ZnAl_2O_4$. Beyond this, no exothermic peak on the DTA curve is observed, indicating that no recrystallization of $ZnAl_2O_4$ spinel occurs up to temperature 1000°C. This result shows a good thermal stability of the spinel structure of $ZnAl_2O_4$ phase at high temperature; a fundamental property for use as catalyst support in reactions at high temperatures. This result is well in agreement with the XRD results.

3.2 X-ray Diffraction (XRD)

The XRD pattern of the as-prepared (a) and heat treated sampless calcined at 600°C (b), 700°C (c), 800°C (d) and 900°C (e) for 4h is shown in Figure 4. From the XRD pattern of as-prepared sample, it seems to be a mixture of aluminium hydroxide and zinc hydroxide with a non-cubical structure [40]. The XRD pattern of the sample calcined at 600ºC for 4h shows that the peaks of mixture of aluminium hydroxide and zinc hydroxide vanished and four new broad peaks appeared at 2θ ~ 31.38°, 36.96°, 59.42° and 65.56° with d values 2.848 Å, 2.430 Å, 1.554 Å and 1.432 Å, respectively; which are the main XRD peaks of a spinel structure [38]. The broad XRD peaks indicate formation of poorly crystallized $ZnAl_2O_4$ develops at 600ºC for 4h. When the sample calcined at 700°C for 4h, the four peaks slightly shifted, sharpens and appeared at 2θ ~ 31.44°, 37.04°, 59.56° and 65.52° with d values 2.843 Å, 2.425 Å, 1.551 Å and 1.432 Å, respectively. Besides, two very weak diffraction peaks appeared around 2θ ~ 45.10°, 55.86°. This XRD pattern matches with peaks of γ -Al_2O_4 [JCPDS 77-0396]. This is an intermediate phase of cubic spinel structure (a rock-salt type structure) [41].

When calcination temperature was increased to 800ºC, the increase in the peaks height

accompanied by sharpening of characteristics diffraction peaks at 2θ ~ 31.28° (220), 36.86° (311), 44.88° (400), 55.68° (422), 59.38° (511) and 65.36° (440) with d values 2.857 Å, 2.436 Å, 2.018 Å, 1.649 Å, 1.555 Å and 1.427 Å, respectively. The XRD pattern is compared with $ZnAl_2O_4$ cubic spinel [JCPDS 74-1138].

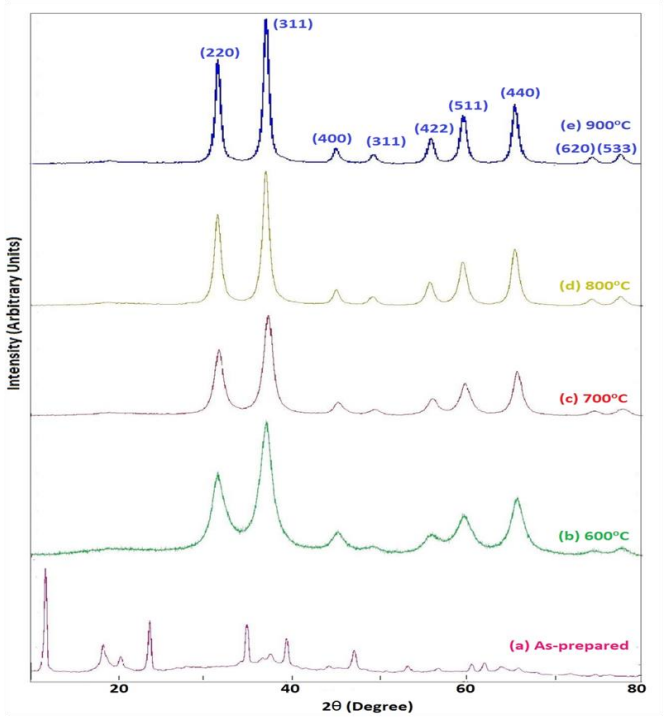

Figure 4 : XRD patterns of as-prepared and thermally treated samples of zinc aluminate at different temperatures for 4h.

All the diffraction peaks are found in good match with the reported results and structure and the peaks are indexed accordingly. All peaks are well defined and pointing to the high crystalline nature of the single-phase $ZnAl_2O_4$ spinel having (311) as the preferential orientation.

Finally, for calcination at 900°C for 4h, the diffraction peaks become stronger, sharper, well defined and can be precisely indexed to face-centered cubic spinel-structured $ZnAl_2O_4$. In addition, no impurities were detected in the synthesized sample. This result suggests the growth in size & crystallinity and single-phase face-centred cubic $ZnAl_2O_4$ nanopowder can be obtained by coprecipitation method followed by heat treatment at 900°C for 4h. Recalling, spinel-type cubic structure, which is traditionally, divided into two different ideal structure types, normal and inverse. In normal spinels, divalent ions of spinels are solely located on tetrahedral sites and trivalent ions solely on octahedral sites within the Fd3m space group. Inverse spinels have half of the trivalent ions residing on tetrahedral sites, while the rest of the trivalent ions and all the divalent ions occupy the octahedral sites. At the nanoscale, the cation distribution is often found to be mixed (between these two ideal structure types), and this is then quantified by the inversion parameter, which corresponds to the fraction of divalent ions residing on the octahedral sites. Thus, in order to get details of the structural and microstructure parameters of the prepared $ZnAl_2O_4$ spinel nanopowder, diffraction data are further examined.

Effects of heat treatment on structure parameter of $ZnAl_2O_4$ like lattice constant, spinel phase, crystallites size and microstrain and dislocation density have also been discussed.

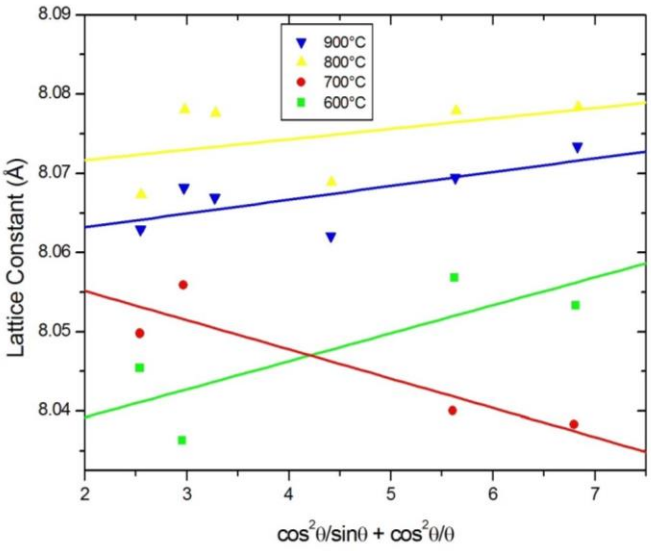

Figure 5: Lattice constant (calculated from Miller indices and interplanar spacing) versus Nelson-Riley function.

In the present work, lattice constant of $ZnAl_2O_4$ crystallites is calculated by Nelson-Riley function, because this function eliminates the error in lattice constant due to sample displacement [42]. Figure 5 displays plot between lattice constant and Nelson-

Riley function. Value of lattice constant for different calcination temperatures is obtained from the intercept of the straight line and represented in Table 1.

It is noticed that lattice constant of $ZnAl_2O_4$ calcined powders is smaller than that of the bulk (lattice constant~8.098Å) and this could be due to size effect [43].

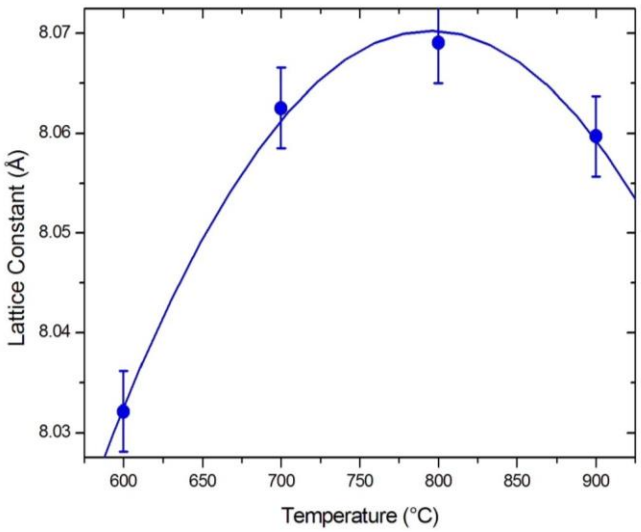

Figure 6 : Lattice constant versus annealing temperature

In Figure 6, the change of the lattice parameter with thermal heating is shown. The lattice parameter of the sample shows a polynomial dependence on calcination temperature. Lattice parameter changes are mainly due to: (i) simple thermal expansion, and (ii) the changes in the cation distribution. The trend of lattice parameter with increasing calcination temperature could be due to zinc (Zn^{2+} ~ 0.74 Å) and aluminium (Al^{3+} ~ 0.53 Å) ionic radii involved in cation rearrangement between the octahedral and tetrahedral sites in the spinel [44]. In general, the ionic radii of divalent ions are, larger than the trivalent ions, where as the tetrahedral sites are smaller than octahedral sites. Therefore, it would be reasonable that the trivalent ions could reside in the tetrahedral/ octahedral sites or into both sites but the divalent ions would prefer to go into the octahedral sites.

Practically, tetrahedral and octahedral interstitial sites of spinel are not fully occupied by their preferred divalent and trivalent cations. A fraction of cations occupy interstitials sites as anti-site cations. The arrangements of cations between interstitial sites depend on synthesis method and post treatments; to name a few, temperature, and pressure and ion irradiation [45]. The re-equilibrate of distribution of cations is one of responsible mechanisms for ordering-disordering in spinels and as a result structural parameters of spinel changes and hence its properties also [46]. The order-disorder process in spinel is termed "non-convergent," since there is no symmetry change upon disordering and a completely disordered state is approached asymptotically with increasing temperature. In the present study, lattice constant increases with increasing temperature upto 850°C and then a sudden change in lattice constant with temperature is due to ordering-disordering transformation in the spinel.

In general, grain size of nanostructured materials can be estimated by Debye-Scherrer equation and size-strain plot. The Debye-Scherrer equation is:

$$D_{D-S} = \frac{\phi\lambda}{\beta\cos\theta} \qquad (1)$$

Where D_{D-S} is the average grain size of the phase under investigation, ϕ is the Scherrer constant and taken to be ~ 0.9, λ is the wave length of X-ray beam used, β is the full-with half maximum (FWHM) of diffraction and θ is the Bragg's angle.

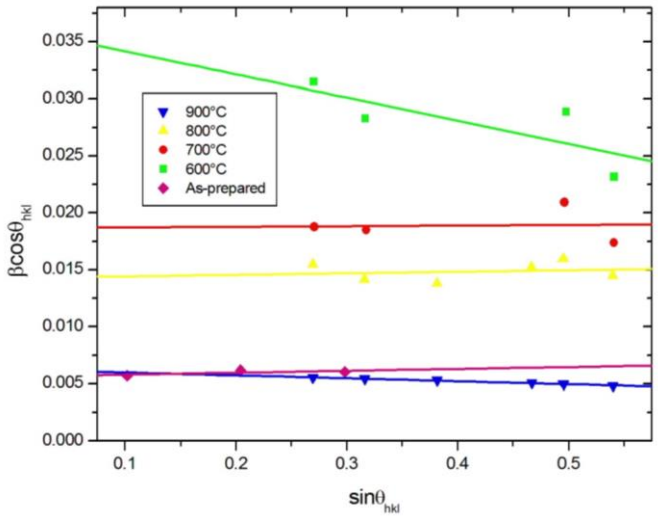

Figure 7 : Williamson-Hall plot of calcined of $ZnAl_2O_4$ spinel nanopowders

It is well known fact that the grain size and micro-strain produces peak broadening in the diffractogram. This could be due to the stresses and faults inside the prepared spinel nanoparticles. The grain size and the strain effect have to be differentiated in the diffractogram. Both effects are independent and can be distinguished by size-strain plot. This size-strain plot is also known as Williamson-Hall plot (W-H plot).

Using W-H plot, size and micro-strain of the grain are estimated simultaneously. The W-H equation is:

$$\beta_{hkl}Cos(\theta_{hkl}) = \frac{K\lambda}{D_{WH}} + 2\varepsilon Sin(\theta_{hkl}) \qquad (2)$$

Where K is the shape factor, λ is the wavelength of X-ray, θ_{hkl} is the Bragg angle, ε is the micro-strain and D_{W-H} is average grain size measured in a direction perpendicular to the surface of the specimen. The graph is plotted between $Sin(\theta_{hkl})$ and $\beta_{hkl}Cos(\theta_{hkl})$ as shown in Figure 7. The value of micro-strain is obtained from slope of the fitted line, whereas value of grain size is obtained from the intersection with the vertical axis. By fitting the data, the average grain size (D_{W-H}) and micro-strain (ε) are estimated and given in Table 1.

The plot of grain size versus calcination temperature is shown in Figure 8. Grain size increases almost linearly with increasing calcination temperature. A $ZnAl_2O_4$ cubic spinel nanopowder with good yield is obtained by the heat treatment at temperature 900°C for 4h.

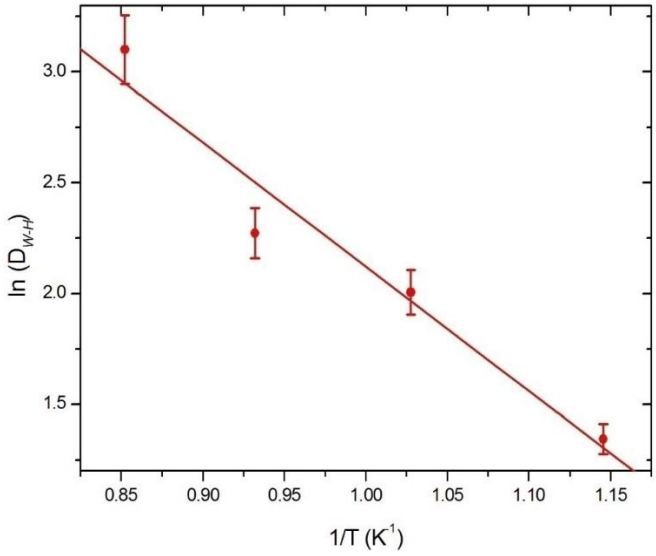

Figure 8 : Crystallite size versus calcination temperatures for 4 h.

The activation energy for formation of $ZnAl_2O_4$ cubic spinel is found to be 47kJ/mol, which is smaller than that of its bulk form (activation energy in the range 80-400 kJ/mol.). Further, by knowledge of average grain size and an empirical relation $\rho \cong \frac{1}{D_{XRD}^{\ 2}}$, dislocation density of $ZnAl_2O_4$ cubic spinel nanocrystallites is calculated and given in Table 1. When calcination temperature is increased, the density of dislocation decreases because of less nucleation sites is available during crystallization, and eventually a large final crystallite size is obtained.

Table 1

Calcined Sample	Crystallite size $D_{D\text{-}S}$ (nm)	Crystallite size $D_{W\text{-}H}$ (nm)	Strain (ε)	Lattice constant (Å)	X-ray density (g/cm³)	Dislocation density $\rho \cong \frac{1}{D_{XRD}^{\ 2}}$
600°C (4h)	4.90	3.83	1.01 x10^{-2}	8.0321	4.669	0.0682
700°C (4h)	7.50	7.43	2.72 x10^{-4}	8.0625	4.616	0.0181
800°C (4h)	9.80	9.71	6.75 x10^{-4}	8.0691	4.605	0.0106
900°C (4h)	25.49	22.20	1.28 x10^{-3}	8.0597	4.621	0.0020

3.3 Fourier Transform Infrared Spectroscopy (FTIR)

FTIR spectroscopy provides valuable information about the phase composition and bonding in a

sample. The FTIR of samples; as-prepared (a) and calcined samples 600°C (b), 700°C (c), 800°C (d) and 900°C (e) for 4h is shown in Figure 9, within the spectral range of 4000-400 cm^{-1}.

FTIR spectrum of as-prepared sample shows three distinct strong absorption bands centered around 1384, 1636 and 3467 cm^{-1}. The absorption band centred around 1383 cm^{-1} could be ascribed for presence of nitrate groups [47]. The bands around 3466 cm^{-1} and 1636 cm^{-1} could be assigned as the stretching vibration of H-O-H molecule and the bending modes of H-O-H absorbed at surface of the product, respectively [48]. The stretching vibration of H-O-H molecules overlaps with surface hydroxyl group vibrations and as a result the stretching band broadens [49]. A broad band noted around 554 cm^{-1} may be assigned as mixture of hydroxide of zinc and aluminium [50]. FTIR of sample (b) shows two distinct signatures : (i) an evaporation of nitrate group which is manifested by elimination of the absorption band centred around 1383 cm^{-1} and this signature confirms decomposition of nitrates; (ii) the metal oxide band is splitted in three weak bands and appeared around ν_1=685 cm^{-1}, ν_2=561 cm^{-1} and ν_3=499 cm^{-1}, ν_1 could be assigned as AlO_4 group [51], where ν_2 and ν_3 could be assigned to AlO_6 group and Zn-O stretching vibrations, respectively [52-54].

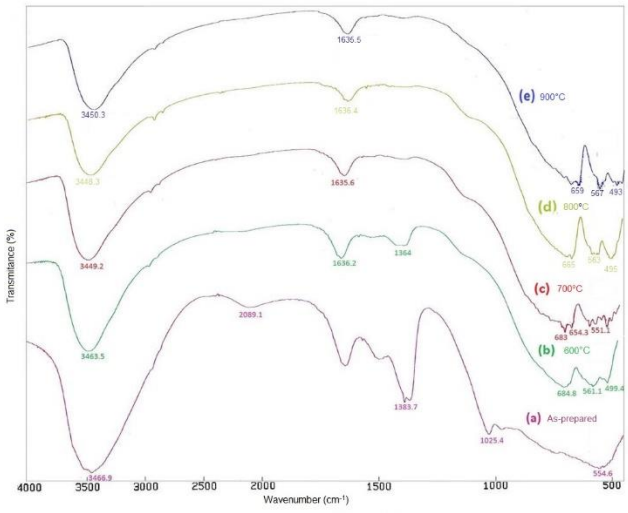

Figure 9 : FTIR spectra of as-prepared and thermally treated samples of zinc aluminate at different temperatures for 4h

This data supports XRD results and confirms the presence of some of Al^{3+} in both the tetrahedral and octahedral sites. At 700°C, the absorption band centred around 1383 cm^{-1} completely disappeared which confirms elimination of nitrate groups. FTIR of the sample (c) displays strengthening in absorption band of AlO_6 and ZnO. This FTIR spectrum also reveals a significant decrease in percentage of evaporation surface water molecules. At relatively higher calcination temperatures 800°C (4h) and 900°C (4h), the tetrahedral and octahedral sites band become sharper due to the minimization of lattice distortion and enhancement of crystallinity (reduction of surface effect). The FTIR results are in close agreement with XRD studies. Here it is worth pointing out that even at temperature 900°C for 4h, some OH groups (3450 cm^{-1} and 1640 cm^{-1}) remains in the structure. This small amount of water molecules could be due to the inter absorption during the compaction of powder specimen with KBr.

3.4 Scanning Electron Microscopy (SEM)

The surface morphology of calcined samples was investigated by SEM equipped with EDS. Micrographs of heat treated sample at different temperatures are shown in Figure 10. The morphology of the sample annealed at 600°C (4h) shows agglomerated particles with various shapes such as spheroidal, rectangular and platelet (Figure 10a). Micrograph (10b) exhibits microstructure of the intermediate phase of cubic spinel zinc aluminate with excess aluminium oxides while micrograph (10c) reveals morphology of well formed $ZnAl_2O_4$ cubic spinel. The micrograph (10d) of the sample calcined at 900°C for 4h displays similar to superposed platelet structure with no definite grain size of $ZnAl_2O_4$ spinel nanopowder with good densification.

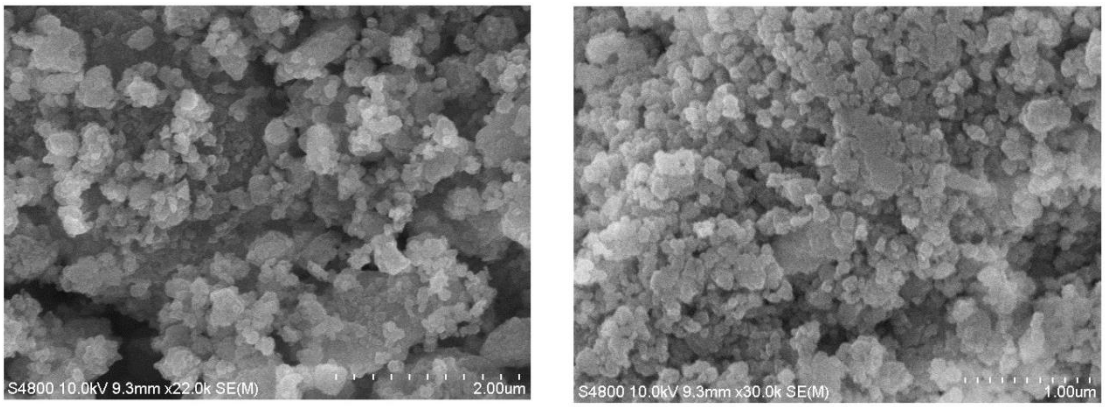

Figure 10a : SEM micrographs of $ZnAl_2O_4$ spinel at calcination temprature 600°C

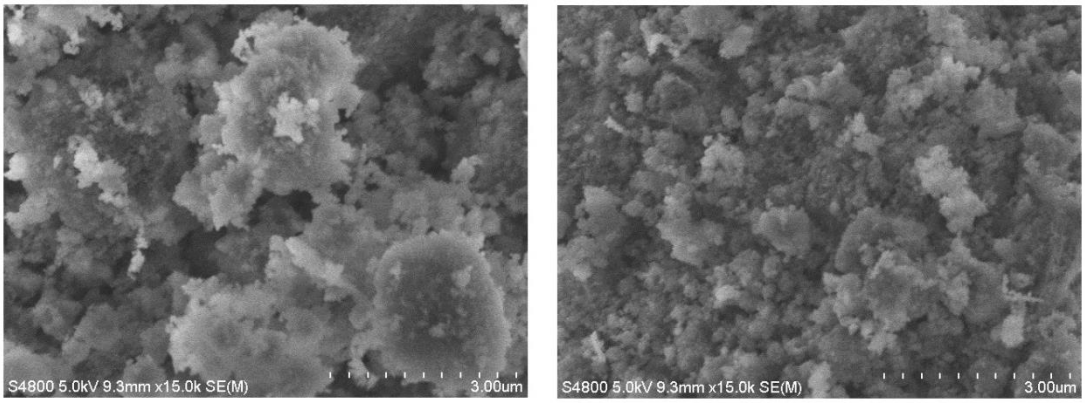

Figure 10b : SEM micrographs of $ZnAl_2O_4$ spinel at calcination temprature 700°C

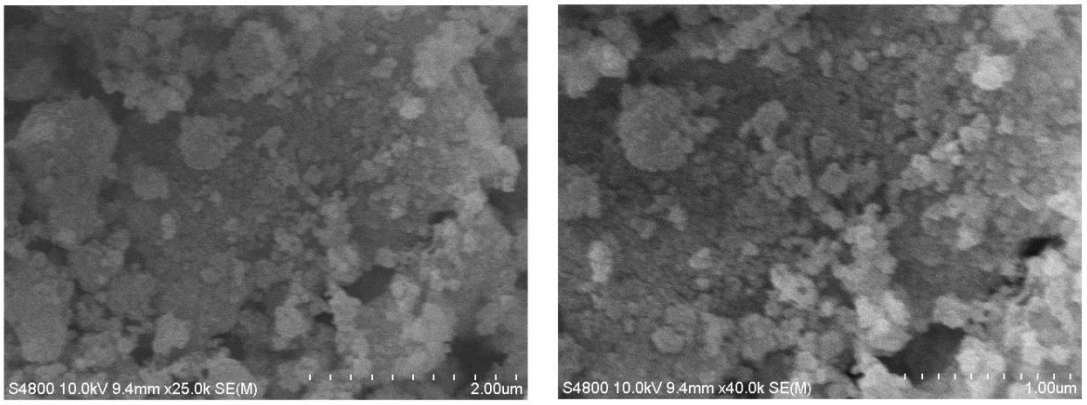

Figure 10c : SEM micrographs of $ZnAl_2O_4$ spinel at calcination temprature 800°C

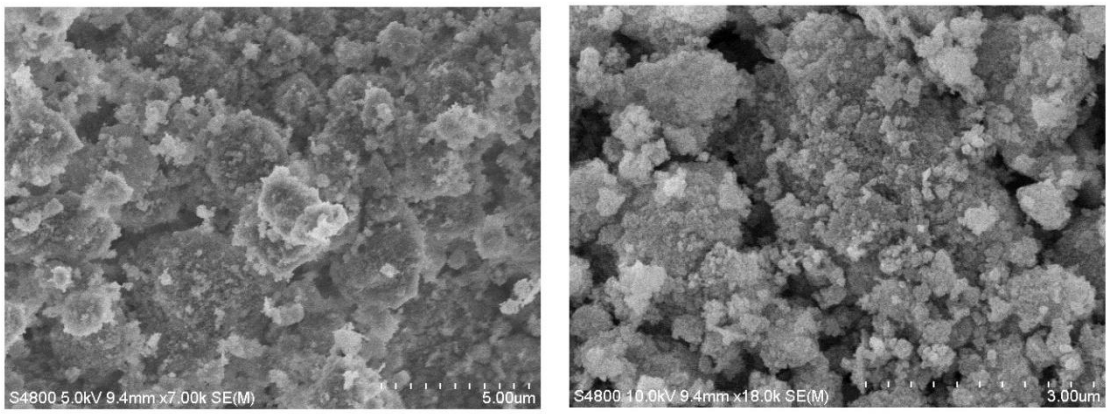

Figure 10d : SEM micrographs of $ZnAl_2O_4$ spinel at calcination temprature 900°C

Figure 11 illustrates the EDS spectrum of the samples and confirms the presence of zinc, aluminium and oxygen. Elemental mapping of heat treated samples showed the presence of only Zn, Al and O in them, the approximate atomic ratio of Zn:Al was found to be ~ 1:2.7. There is an excess of both Al and O ions relative to Zn ions, in $ZnAl_2O_4$ ceramic spinel nanopowder.

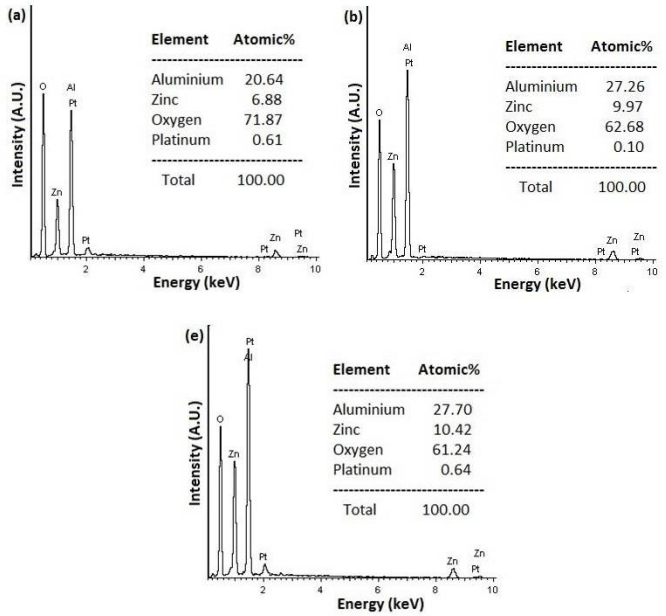

Figure 11: *EDS of samples as-preapred: (a), 700°C: (b) and 900°C : (e)*

IV. SUMMARY

In summary, using precursors: $Zn(NO_3)_2{\cdot}6H_2O$, $Al(NO_3)_3{\cdot}9H_2O$ and ammonia solution, as a precipitating agent, $ZnAl_2O_4$ cubic spinel nanopowder were prepared by coprecipitation method and subsequent thermal heating at temperatures 600°C, 700°C, 800°C and 900°C for 4 hours, in air. The structural properties of $ZnAl_2O_4$ nanopowder were investigated by complementary techniques TGA/DTG/DTA, XRD, FTIR and SEM with EDS. XRD investigations revealed that at calcination temperature 700°C (4h), an intermediate phase (γ-Al_2O_3, a rock salt type structure) of cubic $ZnAl_2O_4$ was formed. In calcination temperature range (700-850°C), interfacial interaction between a high reactive decomposed products γ-Al_2O_3 and ZnO and their mixing at molecular level yielded $ZnAl_2O_4$ face-centred cubic spinel nanopowder with grain size ~ 8 nm. It is also shown that calcination enhances the crystallinity and transmission of the spinel; and also reduces dislocation density and controls amount of stress at the surface and hence yields the strength of the material. Results of TGA-DTG-DTA, FTIR and SEM with EDS support XRD studies. Finally, we may conclude that a single phase $ZnAl_2O_4$ face centred cubic spinel nanopowder (grain size ~ 25 nm) can be obtained by using coprecipitation method followed by thermal treatment at temperature 900°C for 4h, in air. It is expected that the proposed study may find some applications in heavy industry and in particular as catalyst support and catalysts by itself [7-12].

V. REFERENCES

[1]. H. Grabowska, W. Mista, M. Zawadzki and J. Wrzyszcz, Catalytic properties of Fe2O3/ZnAl2O4 system in alkylation reactions of chosen hydroxyarenes with methanol, Polish J. Chem. Technol. 5 (2003) 32-34.

[2]. H. Grabowska, M. Zawadzki and L. Syper, Gas phase alkylation of 2-hydroxypyridine with methanol over hydrothermally synthesised zinc aluminate, Appl. Catal. A : Gen. 314 (2006) 226-232.

[3]. H. St. C. O'neill, M. james, Wayne, Dollase, Simon and T. Redfern, Temperature dependence of the cation distribution in CuAl2O4 spinel, Eur. J. Mineral. 17 (2005) 581-586.

[4]. S. K. Sampath and J. F. Cordaro, Optical Properties of Zinc Aluminate, Zinc Gallate, and Zinc Aluminogallate Spinels, J. Am. Ceram. Soc. 81 (1998) 649-654.

[5]. T. El-Nabarawy, A. A. Attia and M. N. Alaya, Effect of thermal treatment on the structural, textural and catalytic properties of the ZnO-Al2O3 system, Mater. Lett. 24 (1995) 319-325.

[6]. A. Escardino, J. L. Amoros, A. Gozalbo, M. J. Orts and A. Moreno, Gahnite devitrification in ceramic frits: mechanism and process kinetics, J. Am. Ceram. Soc., 83 (2000) 2938-2944.

[7]. J. Wrzyszcz, M. Zawadzki, J. Trawczynsky, H. Grabowska and W. Mista, Some catalytic properties of hydrothermally synthesised zinc aluminate spinel, J. Appl. Catalysis A: General 210 (2001) 263-269.

[8]. J. Zhao, Z. Wang, L. Wang, Hua Yang and M. Zhao, The preparation and mechanism studies of porous titania, J. Mater. Chem. Phys. 63 (2000) 9-12.

[9]. M. A. Valenzuela, P. Bosch, G. Aguilar-Rios, A. Montoya and I. Schifter, Comparison Between Sol-Gel, Coprecipitation and Wet Mixing Synthesis of ZnAl2O4, J. Sol-Gel Sci. Technol. 8 (1997) 107-110.

[10]. A. K. Adak, A. Pathak and P. Pramanik, Characterization of ZnAl2O4 nanocrystals prepared by the polyvinyl alcohol evaporation route, J. Mater. Sci. Lett. 17 (1998) 559-561.

[11]. Y. D. Wang, C. Ma, X. Sun and H. Li, Preparation of nanocrystalline metal oxide powders with the surfactant-mediated method, J. Inorg. Chem. Com. 5 (2002) 751-755.

[12]. A. E. Giannakas, T. C. Veimakis, A. K. Ladavos, P. N. Trikalitis and P. J. Pomonis, Variation of surface properties and textural features of spinel ZnAl2O4 and perovskite LaMnO3 nanoparticles prepared via CTAB–butanol–octane–nitrate salt microemulsions in the reverse and bicontinuous states, J. Coll. Interface Sci. 259 (2003) 244-253.

[13]. H. St. C. O'Neill and A. Navrotsky, Cation distributions and thermodynamic properties of binary spinel solid solutions, American Mineralogist 69 (1984) 733-753.

[14]. N. J. Van der Laag, M. D. Snel, P. C. Magusin and G. de With, Structural, elastic, thermophysical and dielectric properties of zinc aluminate (ZnAl2O4), J. Eur. Ceram. Soc. 24 (2004) 2417-2424.

[15]. M. Valenzuela, J. Jacobs, P. Bosch, S. Reijne, B. Zapata and H. Brongersma, The influence of the preparation method on the surface structure of ZnAl2O4, Appl. Catal. A: Gen 148 (1997) 315-324.

[16]. M. A. Valenzuela, Thesis, ESIQIE-IPN, Me´xico, (1990).

[17]. B. Strohmeier and D. Hercules, Surface spectroscopic characterization of the interaction between zinc ions and γ-alumina, J. Catal. 86 (1984) 266-279.

[18]. I. Ganesh, B. Srinivas, B. Saha, R. Johnson and Y. Mahajan, Microwave assisted solid state reaction synthesis of MgAl2O4 spinel powders, J. Eur. Ceram. Soc. 24 (2004) 201-207.

[19]. M. V. Zdujie´ and O. B. Milosevie´, Mechanochemical treatment of ZnO and Al2O3 powders by ball milling, Mater. Lett. 13 (1992) 125-129.

[20]. D. Domanski, G. Urretavizcaya, F. Castro and F. Gennari, Mechanochemical Synthesis of Magnesium Aluminate Spinel Powder at Room Temperature, J. Am. Ceram. Soc. 87 (2004) 2020-2024.

[21]. L. B. Kong and J. M. Huang, MgAl2O4 spinel phase derived from oxide mixture activated by a high-energy ball milling process, Mater. Lett. 56 (2002) 238-243.

[22]. J. Guo, H. Lou, X. Wang and X. Zheng, Novel synthesis of high surface area MgAl2O4 spinel as catalyst support, Mater. Lett. 58 (2004) 1920-1923.

[23]. L. Chen and X. Sun, Porous ZnAl2O4 synthesized by a modified citrate technique, J. Alloys Compd. 376 (2004) 257-261.

[24]. Y. Wu, J. Du, K. Leong Choy, L. Hench and J. Guo, Formation of interconnected microstructural ZnAl2O4 films prepared by sol–gel method, J. Thin Solid Film 472 (2005) 150-156.

[25]. G. Monro´s and J. Tena, Spinets from gelatine-protected gels, J. Mater. Chem. 5 (1995) 85-90.

[26]. J. Wrzyszcz, M. Zawadzki, A. M. Trzeciak and J. J. Ziółkowski, Rhodium complexes supported on zinc aluminate spinel as catalysts for hydroformylation and hydrogenation:

preparation and activity, J. Mol. Catal. A: Chem. 189 (2002) 203-210.

[27]. M. Zawadzki, W. Mista and L. Kepinski, Metal-support effects of platinum supported on zinc aluminate, Vacuum 63 (2001) 291-296.

[28]. Z. Chen and E. Shi, Synthesis of mono-dispersed ZnAl2O4 powders under hydrothermal conditions, Mater. Lett. 56 (2002) 601-605.

[29]. C. C. Yang, S. Y. Chen and S. Y. Cheng, Synthesis and physical characteristics of ZnAl2O4 nanocrystalline and ZnAl2O4/Eu core-shell structure via hydrothermal route, Powder Technol. 148 (2004) 3-6.

[30]. G. Aguilar-Rios and M. A. Valenzuela, Metal-support effects and catalytic properties of platinum supported on zinc aluminate, Appl. Catal. A: Gen. 90 (1992) 25-34.

[31]. H. Armendariz, A. Guzma´n, A. Toledo, M. Llanos, A. Vazquez and G. Aguilar, In: Morfao J, Faria J, Figueiredo J (eds) Proc. XVII Ibero American symposium of catalysis. Porto, (2000) 105-114.

[32]. J. G. Li, T. Ikegami, J. Lee, T. Mori and Y. Yamija, A wet-chemical process yielding reactive magnesium aluminate spinel (MgAl2O4) powder, Ceram. Int. 27 (2001) 481-489.

[33]. J. Li, T. Ikegami, J. Lee, T. Mori and Y. Yajima, Synthesis of Mg-Al spinel powder via precipitation using ammonium bicarbonate as the precipitant, J Eur. Ceram. Soc. 21 (2001) 139-148.

[34]. Z. Li, S. Zhang and W. E. Lee, Molten salt synthesis of zinc aluminate powder, J. Eur. Ceram. Soc. 27 (2007) 3407-3412.

[35]. A. A. Da Silva, A. de Souza Gonçalves and M. R. Davolos, Characterization of nanosized ZnAl2O4 spinel synthesized by the sol–gel method, J. Sol-Gel Sci. Technol. 49 (2009) 101-105.

[36]. F. Davar and M. S. Niasari, Synthesis and characterization of spinel-type zinc aluminate nanoparticles by a modified sol-gel method using new precursor, J. Alloys and Compd. 509 (2011) 2487-2492.

[37]. A. D. Ballarini, S. A. Bocanegra, A. A. Castro, S. R. de Miguel and O. A. Scelza, Characterization of ZnAl2O4 Obtained by Different Methods and Used as Catalytic Support of Pt, Catal. Lett. 129 (2009) 293-302.

[38]. S. Farhadi and S. Panahandehjoo, Spinel-type zinc aluminate (ZnAl2O4) nanoparticles prepared by the co-precipitation method: A novel, green and recyclable heterogeneous catalyst for the acetylation of amines, alcohols and phenols under solvent-free conditions, Appl. Cata. A: Gen. 382 (2010) 293-302

[39]. H. St. C. O'Neill and A. Navrotsky, Simple spinels; crystallographic parameters, cation radii, lattice energies, and cation distribution, American Mineralogist 68 (1983) 181-194.

[40]. S. A. Bocanegra, A. D. Ballarini, O. A. Scelza and S. R. de Miguel, The influence of the synthesis routes of MgAl2O4 on its properties and behaviour as support of dehydrogenation catalysts, Mater. Chem. Phys. 111 (2008) 534-541.

[41]. J. Bai, J. Liu, C. Li, G. Li and Q. Du, Mixture of fuels approach for solution combustion synthesis of nanoscale MgAl2O4 powders, Adv. Powder Technol. 22 (2011) 72-76.

[42]. A. K. M. Akther Hossain, S. T. Mahmud, M. Seki, T. Kawai and H. Tabata, Structural, electrical transport, and magnetic properties of Ni1–xZnxFe2O4, J. Magn. Magn. Mater. 312 (2007) 210-219.

[43]. G. Li, L. Li, J. Boerio-Goates and B. F. Woodfield, High Purity Anatase TiO2 Nanocrystals: Near Room-Temperature Synthesis, Grain Growth Kinetics, and Surface Hydration Chemistry, J. Am. Chem. Soc. 127 (2005) 8659-8666.

[44]. C. Thiriet-Dodane, Study of irradiation damages in MgAl2O4 and ZnAl2O4 spinels in the framework of nuclear waste transmutation, Report CEA-R-6010-Comunissariat ´al' Energie Atomique France (2002).

[45]. H. St. C. O'Neill and W. A. Dollase, Crystal Structures and Cation Distributions in Simple Spinels from Powder XRD Structural Refinements: MgCr2O4, ZnCr2O4, Fe3O4 and the Temperature Dependence of the Cation Distribution in ZnAl2O4, Phys. Chem. Minerals 20 (1994) 541-555.

[46]. D. Simeone, C. Dodane-Thiriet, D. Gosset, P. Daniel and M. Beauvy, Order–disorder phase transition induced by swift ions in MgAl2O4 and ZnAl2O4 spinels, J. Nucl. Mater. 300 (2002) 151-160.

[47]. K. Vivekanandan, S. Selvasekarapandian and P. Kolandaivel, Raman and FT-IR studies of Pb4(NO3)2(PO4)2·2H2O crystal, Mater. Chem. Phys. 39 (1995) 284-289.

[48]. M. A. Ulibarri, C. Barriga and J. Cornejo, Kinetics of the thermal dehydration of some layered hydroxycarbonates, Thermochim. Acta 135 (1988) 231-236.

[49]. P. Aghamkar, S. Duhan, M. Singh, N. Kishore and P. K. Sen, Effect of thermal annealing on Nd2O3-doped silica powder prepared by the solgel process, J. Sol-Gel Sci. Technol. 46 (2008) 17-22.

[50]. J. Parmentier, M. Richard-Plouet and S. Vilminot, Influence of the sol-gel synthesis on the formation of spinel MgAl2O4, Mater. Res. Bull. 33 (1998) 1717-1724.

[51]. F. Meyer, R. Hempelmann, S. Mathur and M. Veith, Microemlusion mediated sol-gel synthesis of nano scaled MAl2O4 (M = Co, Ni, Cu) spinels from single-Source Heterobimetallic Alkoxide precursor, J. Mater. Chem. 9 (1999) 1755-1763.

[52]. A. K. Adak, S. K. Saha and P. Pramanik, Synthesis and characterization of MgAl2O4 spinel by PVA evaporation technique, J. Mater. Sci. Lett. 16 (1997) 234-235.

[53]. F. Li, Y. Zhaoa, Y. Liua, Y. J. Haoa, R. H. Liua and D. Zhaob, Solution combustion synthesis and visible light-induced photocatalytic activity of mixed amorphous and crystalline MgAl2O4 nanopowders, Chem. Eng. J. 173 (2011) 750-759.

[54]. A. E. Jimenez-Gonzalez, J. A. S. Urueta and R. Suarez-Parra, Optical and electrical characteristics of aluminum-doped ZnO thin films prepared by solgel technique, J. Cryst. Growth 192 (1998) 430-438.

Cite this Article

Dr. Shyam Sunder, Dr. Wazir Singh, "Thermal Evolution of Zinc Aluminate Spinel Nanoparticles Prepared by Coprecipitation Technique", International Journal of Scientific Research in Science, Engineering and Technology (IJSRSET), Online ISSN : 2394-4099, Print ISSN : 2395-1990, Volume 3 Issue 8, pp. 1302-1315, November-December 2017.

Journal URL : http://ijsrset.com/IJSRSET1738233